Journal of Open Aviation Science (2024), Vol.2
doi:10.59490/joas.2024.7899

JOAS

PROCEEDINGS | *The 12th OpenSky Symposium*

Testing Applicability of Point Merge Systems for Göteborg Landvetter Airport

Henrik Hardell [1,2] Tatiana Polishchuk [1] and Lucie Smetanová *,[1]

[1]Linköping University, Norrköping, Sweden
[2]Luftfartsverket (LFV), Norrköping, Sweden
*Corresponding author: lucie.smetanova@liu.se

(Received: 20 Nov 2024; Revised: 14 Mar 2025; Accepted: 25 Apr 2025; Published: 12 May 2025)
(Editor: Manuel Waltert; Reviewers: Rainer Koelle, Annette Temme)

Abstract

The ability to comprehensively evaluate the performance inside Terminal Maneuvering Area (TMA) is important for understanding of the traffic conditions in the airport vicinity, and to identify the areas for possible improvements. We examine performance of the individual arrival flows to Göteborg Landvetter airport and analyze them separately in order to identify the problematic areas. Then, we test the potential of introducing Point Merge (PM) arrival procedure to this airport and schedule aircraft arrivals along them. We aim to determine whether introducing the PM structure improves the arrival performance and analyze the associated trade-offs. Comparing the resulting performance of the optimally-scheduled arrivals with PM against the baseline scenario derived from the historical flight trajectories obtained from the open-source Opensky Network database, we observe that adherence to the PM procedures provides a decrease in the fuel consumption about 5% in average due to improved vertical efficiency, however the time and distance aircraft spend in TMA increased both 10.4%. PM usage provides additional benefits in terms of improved controllability of the traffic flows, supported by significant reduction in the spacing deviation within the control area close to the runway.

Keywords: Terminal Maneuvering Areas; Point Merge; Key Performance Indicators; Arrival Scheduling

Abbreviations: JOAS: Journal of Open Aviation Science, ATM: Air Traffic Management PM: Point Merge TMA: Terminal Maneuvering Area

1. Introduction

Point Merge metering procedures were first introduced by Eurocontrol Experimental Centre (EEC) in 2006 [1] and represent an efficient alternative to classical vectoring techniques to align aircraft into the desired landing sequence. The PM structures are implemented in 44 airports in 20 countries [2] and are becoming more popular around the world as they are known for providing benefits in terms of improved capacity, controllability and environmental efficiency of the arrival operations. There is a certain interest to implement PM in several airports in Sweden, including the two largest Swedish airports of Stockholm Arlanda and Göteborg Landvetter.

Researchers investigated PM systems from different perspectives. Several studies [3, 4, 5, 6, 7] evaluated the potential benefits provided by PM implementation in simulation environments. The authors of [4] presented the results of fast-time simulations for a generic airport comparing arrival operations with vectoring against PM. The results showed that –in comparison to vectoring– the PM model reduces: mean controller task load (20±1%), the number of instructions to pilots (30%), and fuel consumption (170±14 kg). Similarly, real-time simulations for Istanbul International Ataturk Airport with 50 arrivals per hour [3] demonstrated that the average total number of controller instructions is about 33 percent lower and the frequency occupancy is about 37 percent lower for PM than for vectoring.

Better controllability and predictability of the trajectories gained with PM operations were reported during the real-time simulation and validation exercises in Paris Orly airport [6], as well as in simulations at Beijing Capital International airport [5], where the authors of [8] proposed a novel PM design. Simulated annealing was used to optimize the arrival sequence in a busy terminal area featuring a multi-layer PM system, with the aim of efficiently and robustly landing more aircraft by grouping Heavy/Medium/Light aircraft to different layers on the PM sequencing legs. In [7], a newly-designed PM system was proposed for one runway at Amsterdam-Schiphol airport, controlled by a mixed integer programming (MIP)-based arrival management system. A MIP-based optimization was also utilized in [9] for comparison of the different separation requirements for the arrivals performing PM.

In our previous studies, [10, 11, 12] we assessed arrival performance of several TMAs with and without PM structures. In [13] we used clustering technique to calculate arrival performance of individual flows to Stockholm Arlanda airport. We demonstrated that this technique is quite accurate and helps to spot inefficiencies within TMA.

In this work, we evaluate a new PM design for the Göteborg Landvetter airport, the second largest airport in Sweden, to perform a preliminary analysis on whether the PM procedures could improve performance of the arrival flows to this airport. In 2019, the year of interest in this paper, Landvetter handled about 70.000 movements [14] on its single runway 03/21. The airport, situated under Göteborg TMA, operates with both open and closed Standard Arrival Routes (STARs), bringing the aircraft from either of the seven TMA entry points to a fix from which radar vectoring is conducted, or an approach procedure connects directly, respectively. The analysis in this paper is relevant since there is currently an ongoing project on redesigning procedures and TMA for the airport.

2. Performance Evaluation of Current Arrival Operations

In this section, we describe the dataset used for this study and present the methodology for evaluation of individual arrival flows.

2.1 Data

We use historical aircraft trajectories obtained from the OpenSky historical database [15], which provides accurate information about flight movements with the granularity of one second.

For this study, we use arrival data to Göteborg Landvetter airport during April 2019. The year 2019 was historically the year with the highest number of aircraft movements before the Covid-19 pandemics. We choose the month of April for our analysis as it was the busiest month for Göteborg Landvetter airport during the year 2019. The dataset was previously created in our earlier work for investigation of the COVID-19 pandemics impact on arrival performance of the Göteborg Landvetter airport [16], in this work we reused and curated the dataset to fit our purposes. The arrival trajectories were clustered based on the arrival runway and entry point to the TMA using k-means clustering method.

Clustering Technique. We employed the standard k-means clustering approach to group the initial points of aircraft trajectories within the TMA. The k-means method partitions the data into k clusters by iteratively minimizing the total within-cluster variance. Formally, if $X = \{\mathbf{x}_1, \mathbf{x}_2, \ldots, \mathbf{x}_n\}$ is the set of observations and $\boldsymbol{\mu}_1, \ldots, \boldsymbol{\mu}_k$ are the centroids of the clusters $C_1, \ldots, C_k$, then the objective function is:

$$\min_{C_1,\ldots,C_k} \sum_{i=1}^{k} \sum_{\mathbf{x} \in C_i} \|\mathbf{x} - \boldsymbol{\mu}_i\|^2 \tag{1}$$

where $\boldsymbol{\mu}_i$ is the mean of all points assigned to cluster C_i. In our case, we use *Euclidean distance* as the metric $\|\cdot\|$.

Parameters

- **Number of Clusters** (k): We use $k = 6$.
- **Initialization**: Random centroid seeding approach.
- **Convergence Threshold**: The algorithm terminates when centroid movement is below 10^{-4}.
- **Maximum Iterations**: Capped at 300 iterations.

We perform per-cluster analysis, applying the methodology similar to the one proposed for Stockholm Arlanda in [13].

2.2 Performance Evaluation Methodology

The metrics we are using in this study were systematically developed with the goal of evaluation of the TMA performance. We evaluate the vertical and horizontal efficiency as well as the environmental efficiency and metering and spacing using the subset of metrics described in [17]. The subset of metrics used in this work consists of: *Time Flown Level, Vertical Deviation, Horizontal Spread, Distance, Fuel Consumption, Metering and Spacing, Minimum Time to Final, Spacing Deviation, Throughput, Sequencing Effort, PM Utilization, Time in TMA, Additional Time, and ASMA Time.* To better understand the potential of introducing PM procedures, we apply metrics developed specifically to describe the PM structure performance [18]. The dataset was initially established for the purposes of [16] and contains six arrival flows corresponding to the clusters obtained using the outlined clustering method.

We study the following areas using the listed metrics:

- Vertical efficiency
  - *Time Flown Level* - metric which calculates how much time aircraft spent in level-flight, full description in [10].
  - *Vertical Deviation from the Reference Profile* - metric as a function of time to final, defined as the difference in the altitudes between the actual and reference descent profiles, measured as the area under the curve in $ft \cdot minutes$.
- Horizontal efficiency
  - *Horizontal Spread* - metric which gives information on the horizontal usage of the TMA, Equation 6
  - *Horizontal Distance* - the distance flown in TMA.
- Environmental efficiency
  - *Fuel Consumption* - calculated with Equation 7
- Metering and Spacing
  - *Minimum Time to Final* - heatmap of the minimum possible travel times from the current space in TMA to the final. Pseudo-code 1.

  - *Spacing Deviation* - information about the accuracy of spacing between aircraft. Equation 8.
  - *Throughput* - the number of aircraft sharing the same minimum time to final value within a given time window. Pseudo-code 2.
  - *Sequencing Effort* - intensity of the control action applied to organize the aircraft in the desired order for landing. Equation 9
- PM performance
  - *PM Utilization* - which characterizes what part, in percent, of the PM arcs are used by the aircraft.
- Time efficiency
  - *Time in TMA* - metric which indicates the duration aircraft spend in the TMA before landing.
  - *Additional Time* - metric, which measures the time each aircraft spends in TMA beyond the Minimum Time to Final values. Equation 10.
  - *Arrival Sequencing and Metering (ASMA)* - time based on the documentation from Eurocontrol [19] for comparison, but due to lack of data, we adjusted the methodology of ASMA reference time calculation taking into consideration the data for the whole year 2019 instead of the recommended month-11 data.

To study the potential benefits and drawbacks of introducing PM design, we apply the methodology proposed in our previous work [20] for scheduling arrival flows along the proposed PM structures. We apply the optimization framework for assigning the optimal, conflict-free set of arrival routes, given a real traffic scenario, obtained from historical flight data. Moreover, in case of single-runway or mixed-mode operations, the framework considers the synchronization between arrivals and departures at the runway, providing necessary additional spacing when required to allow aircraft to safely take off. Then we evaluate the resulting performance using the metrics introduced earlier in this section.

3. Analysis Per Flow/Cluster

We analyze the arrivals to Göteborg Landvetter airport during April 2019, performing the calculations per flow.

Figure 1 corresponds to the flight trajectories for each cluster. The trajectories are clustered based on the position of their entry to TMA to assure fair evaluation of the traffic flows and the TMA performance. Figure 1 illustrates clearly that the distance aircraft spend inside TMA significantly differs between the six clusters, since the runway is not centered within the TMA. As a result, the time aircraft spend inisde TMA will also differ. The Horizontal Spread values are quite disperse among the clusters as clusters arriving from southern part of the TMA travel shorter distance to the runway than the trajectories arriving from north-eastern part of the TMA. The Horizontal Spread values vary between 5.75% for cluster 4, which only contains five flights, and 35.98% for cluster 2. The average Horizontal Spread among the clusters is approximately 13%, highlighting the high Horizontal Spread value for Cluster 2 as an outlier.

Figure 2 shows the Minimum Time to Final visualization through heatmaps for each of the clusters. The Minimum Time to Final metric follows similar trend with the highest maximum value 1378 seconds for Cluster 2 and smallest maximum value of 603 seconds for Cluster 6. The range of the Minimum Time to Final values can be observed using the color scale towards the right side of each line of the figures, the scale is unified for all clusters.

Figure 3 shows the evolution curves of the Spacing Deviation metric for each cluster. The curves feature similar shape for most of the clusters, with the difference for Cluster 2 where the higher dis-

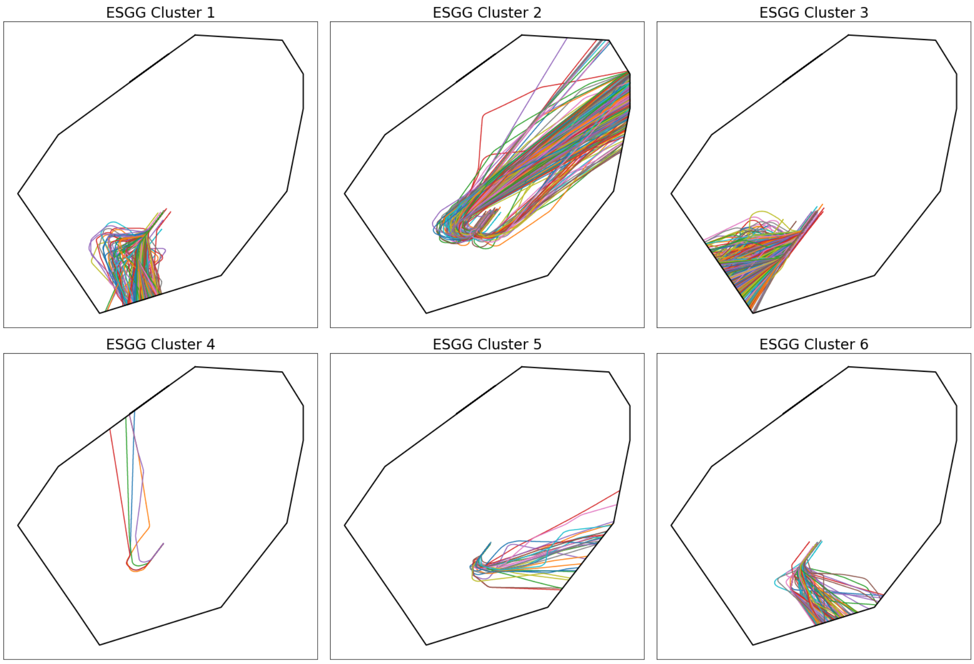

Figure 1. Trajectory plots for six clusters of the aircraft arriving trajectories at Göteborg Landvetter airport in April 2019.

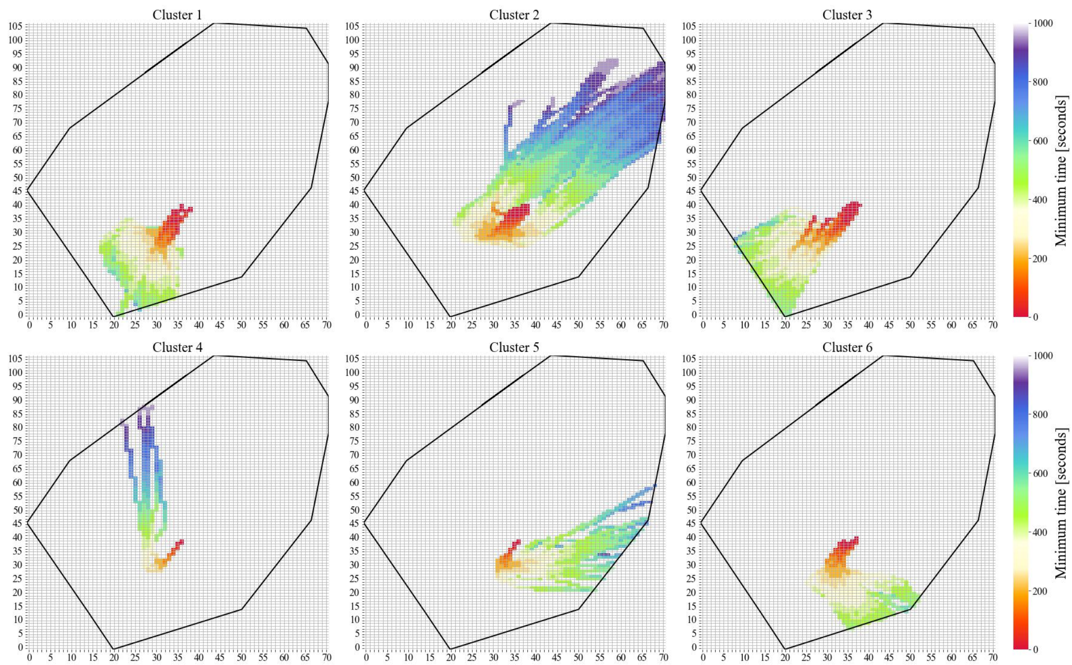

Figure 2. Minimum Time to Final heatmaps for six clusters of the aircraft arriving trajectories at Göteborg Landvetter airport in April 2019.

persion around 500 seconds to final suggests that maintaining the spacing between the consecutive aircraft pose a challenge to ATM. The low dispersion of the curves around 70 seconds to final for all clusters indicates successful sequencing before the final approach (even earlier, around 100 seconds for clustera 1, 3 and 4). Table 1 shows the number of flights in each cluster. We notice that despite clusters 1, 3, and 6 contain a different number of arrivals, the 90^{th}-quantile width for the Spacing Deviation is similar for them: 176, 211, and 168 for clusters 1, 3, and 6 respectively. This implies that traffic flows were well organized even during high-traffic periods.

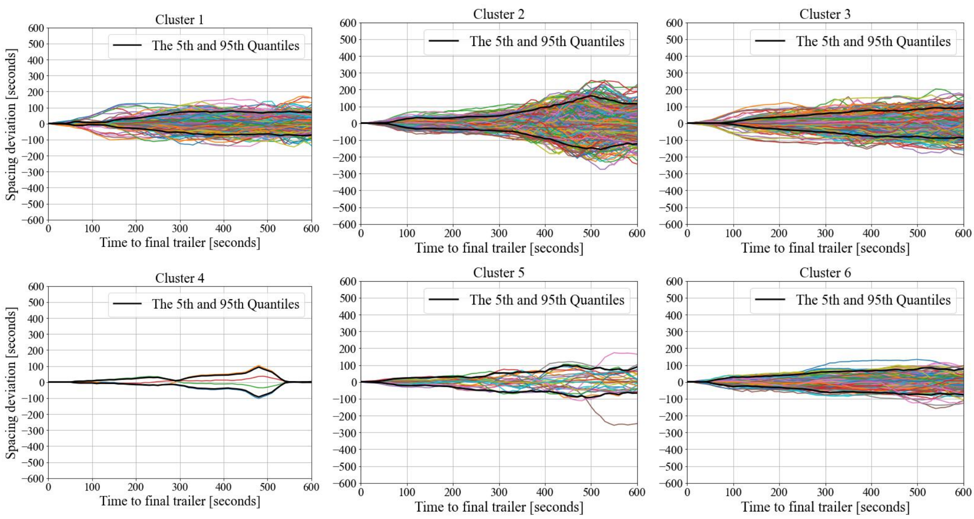

Figure 3. Spacing deviation evolution lines for six clusters of arriving trajectories to Göteborg Landvetter airport in April 2019.

Table 1. Number of flights per cluster

	Cluster 1	Cluster 2	Cluster 3	Cluster 4	Cluster 5	Cluster 6
Number of flights	363	429	566	5	31	139

Sequencing Effort for each of the clusters is illustrated in the second two rows of Figure 4. The Sequencing Effort shapes highlight the peaks in the Spacing Deviation values which is visible especially well for clusters 2 and 4. The highest control action was applied for Cluster 2 with maximum value of 183, the average values of Sequencing Effort range between 27 for Cluster 4 and 101 for Cluster 2. The smallest average value of the Sequencing effort for Cluster 4 confirms that the flow is well-organized in this cluster and does not require much control effort, while busy Cluster 2 requires significantly more attention.

The Vertical efficiency metric Time Flown Level values for each cluster are presented in Figure 5 - (a). The time on level values are similar for most of the clusters, Cluster 2 experiences higher dispersion with many outliers. Despite the low number of arrivals, the aircraft in Cluster 4 spent significantly more time on levels than the ones from other clusters, demonstrating significant vertical inefficiency, which should be investigated further.

Figure 5 - (b) shows the comparison for the Additional Time and the standardized ASMA additional time metrics for the three busiest clusters. The comparison is shown only for Clusters 1, 2, and 3, because the ASMA reference time for the other clusters does not satisfy the algorithms conditions (the number of aircraft in the clusters is too low). We can see that despite the reference time calculation is remarkably different for the two approaches, the resulting values demonstrate similar trends. Aircraft in Cluster 2 spend significantly more time in TMA because of the asymmetric TMA

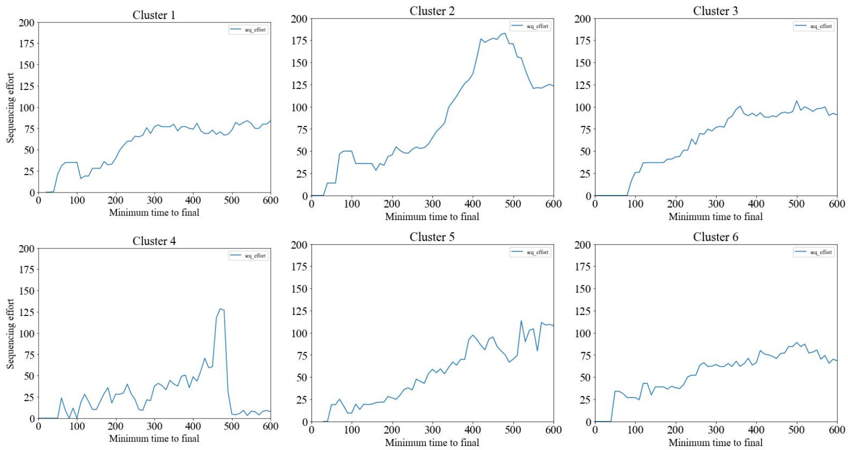

Figure 4. Sequencing Effort curves for six clusters of arriving trajectories to Göteborg Landvetter airport in April 2019.

geometry, with the runway positioned not exactly in the center of the TMA, with the furthest from the runway entry to TMA for Cluster 2 in comparison to other clusters.

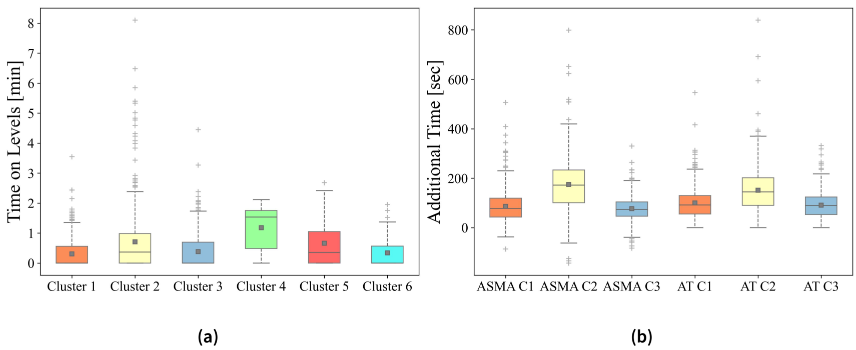

Figure 5. Statistics for the Time Flown Level metric for six clusters (a) and comparison of ASMA additional time and the Additional Time metrics for three clusters (b).

4. Point Merge Simulation

In order to investigate the potential benefits of introducing PM at the airport, we use a recent design that has been tested within an ongoing airspace and procedure modernization program for the airport. We, as a research group, interpret ourselves how to operationally use the design with the arriving traffic, and only use the design proposal itself as an inspiration.

The proposed solution contains two single arcs with traffic flow in one direction, as illustrated in Figure 6. Since the design does not contain overlapping legs, we do not enforce a level-flight requirement along the sequencing legs, and hence, allow for a continuous descent. We set a speed limit of indicated airspeed (IAS) 220 kt along the sequencing legs and a 200 kt restriction upon reaching the intermediate approach fix (IF), which is to be crossed at an altitude of 3000 ft. The descent from 3000 ft along an ILS approach starts at approximately 3.5 NM from the IF.

4.1 Arrival Optimization

We evaluate the potential benefits of introducing PM at the airport by utilizing an optimization framework, previously used to successfully schedule arrivals during busy-hour periods at both Dublin and Oslo-Gardermoen airports [13],[20]. In this paper, we will provide a general overview of the main components, and refer to the two aforementioned references for more detailed information.

We start by discretising the sequencing legs by introducing additional waypoints from which an aircraft may turn towards the merge point. In between every waypoint (E1-E6 and W1-W6, shown in Figure 6), we create two additional waypoints, equally spaced in between each pair of existing waypoints. In total, this results in 16 points along each arc. Aircraft joining an arc at E6 or W6 will be able to use any of the 16 points per arc as a turning point, while aircraft joining via E3 and W3, or E1 and W1, will have seven and one available turning points, respectively.

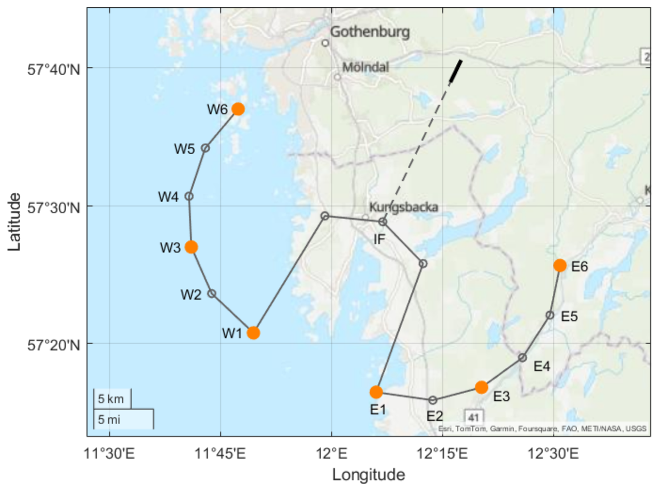

Figure 6. Proposed PM design and its geographical location. Waypoints in orange represent waypoints at which aircraft may join the PM arcs.

For constructing aircraft feasible trajectories, we assign the point (E1, E3, E6, W1, W3 or W6) at which each aircraft shall join an arc, based on the direction from which arriving aircraft enter the TMA, and make a direct route from TMA entry to the selected arc waypoint. In case E1 or W1 are assigned as the arc entry point, we create additional route options for entering via E3 or W3 for the specific aircraft, in order to allow for more than one possible route.

We use a variety of different data sources for the creation of arrival routes. Opensky Network [15] for historical ADS-B data, ECMWF ERA5 reanalysis data [21] on different atmospheric variables and Eurocontrol Base of Aircraft Data (BADA) v4.2 [22] for aircraft performance modeling. These components are used in our trajectory prediction model.

Next, we analyze the historical trajectories of all flights present in the TMA using the dataset extracted from Opensky Network, for the period during which we intend to apply arrival optimization. Note that this includes trajectories for both arriving and departing aircraft, since also the number of aircraft taking off will affect the capacity of the single runway. For the arriving traffic, we obtain aircraft type, the time at which the TMA is entered, cruise altitude, as well as calculate the TMA entry speed, converted from ground speed (GS) to calibrated airspeed (CAS) using the prevailing atmospheric conditions, obtained from the ERA5 reanalysis dataset, provided via the C3S Data Store [21]. More specifically, we use historical data on temperature, wind direction, and wind speed at different altitudes and positions and apply linear interpolation in position and time to make estimations in between the forecasted grid points. For the departing aircraft, we obtain aircraft type and timestamp of the first registered point of the trajectory.

We use BADA together with atmospheric data from the ERA5 reanalysis dataset for modeling the performance of the arriving aircraft at a weight of 90% of the maximum landing weight (MLW). In case the actual aircraft type is not available, we select a type of similar size and performance. We assume a continuous descent operation (CDO) with the engines operating at idle thrust, where the descent angle of the aircraft depends on the selected speed. For the descent speed profile, we match the CAS of the actual aircraft at TMA entry (obtained and calculated from the OpenSky data) and enforce a 250 kt speed limit below FL100. As stated in Section **??**, we introduce additional speed requirements of 220 kt and 200 kt along the sequencing legs and at the IF, respectively. The rate of descent during each second of the trajectory is obtained via the total energy model (TEM) in Equation 2. We build the vertical trajectory backwards, starting from the IF, for the different route options that are available to each aircraft. When generating the vertical trajectory backwards, we set the trajectory to maintain level flight in case the cruise altitude of the actual aircraft is reached before the horizontal trajectory reaches the TMA border. Finally, we adjust the trajectory to match the actual TMA entry time of the actual flight. Each arrival route, assigned time information, we call an arrival profile.

$$(Th - D) \cdot V_{TAS} = m \cdot g_0 \cdot \frac{dh}{dt} + m \cdot V_{TAS} \cdot \frac{dV_{TAS}}{dt} \tag{2}$$

Here, Th is the thrust force, D is the drag force, V_{TAS} is the true airspeed, m is the aircraft mass and g_0 is the gravitational acceleration.

In terms of separation, we apply the time-based separations proposed in [23] between an arrival and an arrival, and between an arrival and a departure at the runway threshold. Since the optimized arrival routes end at the IF (to be connected with the published ILS approach [24] from this point), we make an estimation on the average flight time between the IF and the runway threshold, a distance of 11.25 NM. We assume an average GS of 180 kt, which results in a flight time of 225 s.

4.2 Optimization Framework

We apply the framework, based on the mixed-integer programming (MIP), proposed in [12], [20]. MIP is an optimization technique that involves both continuous and discrete decision variables, allowing it to model complex combinatorial problems. It is widely used in air traffic management problems to find optimal solutions while satisfying operational constraints. The framework provides the optimal assignment of arrival routes for each aircraft, ensuring safe time separation between aircraft at all waypoints, as well as synchronization between arrivals and departures at the runway.

Prior to running the optimization, we check for conflicts between the set of all available arrival profiles, i.e. which arrival profiles do not respect the time separation requirement. Such arrival profile pairs are stored in a matrix. Then, this matrix is used as an input to the optimization model described in detail in [12], [20], which ensures that two conflicting profiles are not selected simultaneously, that each aircraft is assigned only one profile, and that sufficient spacing is provided between aircraft landing and taking off, whether the arriving aircraft lands prior to or after the departing aircraft. We set the objective function to minimize the total fuel consumption of all arriving aircraft, according to Equation 3. Equation 4 ensures that two conflicting profiles are not selected simultaneously, while Equation 5 ensures that each aircraft is assigned only one profile.

$$\min \quad \mathcal{J} := \sum_{a \in \mathcal{A}} \sum_{p \in \mathcal{P}_a} x_{a,p} \cdot F_{a,p} \tag{3}$$

$$x_{a_i,p_k} + x_{a_j,p_r} \leq 1, \ \forall a_i, a_j \in \mathcal{A}, \ \forall p_k \in \mathcal{P}_{a_i}, \ \forall p_r \in \mathcal{P}_{a_j} \\ \mid ((a_i, p_k), (a_j, p_r)) \in \mathcal{I} \tag{4}$$

$$\sum_{p \in \mathcal{P}_a} x_{a,p} = 1, \quad \forall a \in \mathcal{A} \tag{5}$$

a represents an individual aircraft in the set A, containing all aircraft scheduled to arrive, while p represent an arrival profile in the set of all available arrival profiles for aircraft a, p_a . $x_{a,p}$ and $F_{a,p}$ are a binary variable indicating whether aircraft a is assigned profile p, and the fuel burn of the corresponding profile, respectively. In addition to the two constraints stated above, the formulation of the optimization problem contains a couple of constraints which ensure that arrivals and departures can operate on the runway without conflicts, and provides necessary additional spacing between arrivals to allow an aircraft to take off.

4.3 Experimental Evaluation

In this section, we describe the dataset used to evaluate the optimized PM arrivals, as well as the corresponding results on time in TMA, distance, vertical deviation, fuel consumption, and spacing and sequencing.

4.3.1 Dataset

We choose to evaluate the PM design on the busiest day of April 2019, with 90 arrivals in total. The aircraft mix during this day consists of 84 wake turbulence category (WTC) Medium (M) aircraft and six WTC Heavy (H) aircraft. In addition, there are 95 departing aircraft, out of which 91 belong to WTC M and four to WTC H. Figure 7 (a) shows the actual arrival routes for the flights on April 10, 2019, colored according to cluster belonging, while Figure 7 (b) shows all possible arrival routes that were created for the optimized scenario with PM, 988 in total. Note that we added two additional waypoints located 3 NM from either arc, in order to prevent unacceptably sharp turns for some traffic entering in the middle of a PMS. The deconfliction step is performed on a standard laptop in Matlab in less than one min, while the optimization itself is solved in less than 5 s. The optimization problem is implemented in AMPL and then solved with the Gurobi Optimizer [25]. Gurobi Optimizer is a state-of-the-art mathematical optimization solver that efficiently handles linear, integer, and quadratic programming problems using advanced algorithms such as simplex, barrier, and branch-and-bound. The dataset contains 1407 conflicts in total, meaning there are 1407 arrival profile pairs that do not satisfy the separation requirement.

The position of the first timestamp for departing aircraft in our dataset varies. Some aircraft are detected already at the start of the takeoff roll, while other aircraft first need to gain some altitude. In order to make an estimation on the actual takeoff time, we assume that lift-off occurs at 2000 m after the beginning of the runway, after a takeoff roll with a duration of 30 s. In case the aircraft has not yet lifted off the runway at the time of the first timestamp, we make an interpolation along the runway to estimate the actual takeoff time. In case the aircraft is first detected in the air, we assume an average GS of 180 kt from the 2000 m location, refereed to above, and estimate the actual takeoff time by deducting a 30 s takeoff roll and the time of travel in the air, from the first timestamp.

4.3.2 Optimized Arrival Schedule

The actual arrival routes inside TMA, cut at the location closest to the IF in the proposed PM design, are shown in Figure 8 (a), while Figure 8 (b) illustrates the resulting arrival routes output from the

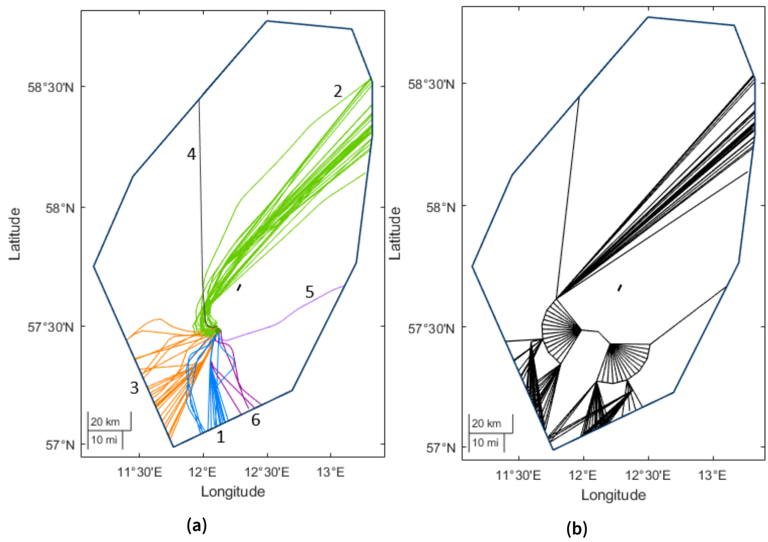

Figure 7. Actual arrival routes with cluster assignment illustrated by color (a) and available arrival routes to use within the optimization framework (b).

optimization framework, with ten aircraft scheduled to use PM arcs to some extent for sequencing purpose. The rest of the aircraft can proceed directly to the merge point after passing the PM arc entry point. Due to a separation conflict between two aircraft at waypoint W6 (Figure 6), which cannot be resolved by using PM sequencing legs, one aircraft had to be adjusted (delayed) by 90 s, meaning that its time of arrival at the TMA border is 90 s later compared to that of the actual flight. In Figure 9, we show how the number of movements in the optimized scenario with PM is spread across the hours of the day, observing a variation between one movement in the very early morning and 18 movements at maximum between 07:00-08:00. Figure 10 shows the timeline of the runway utilization for the optimized arrivals using PM, indicating also which flights actually used the sequencing legs for path stretching (shown as a vertical line below the dot indicating the arrival time.) Out of the ten aircraft using the sequencing legs, three occurred between 06:00 and 07:00, two between 07:00 and 08:00, one between 15:00 and 16:00, one between 16:00 and 17:00, and three between 19:00 and 20:00. Note that all times are expressed as Coordinated Universal Time (UTC). Local time at Göteborg-Landvetter is UTC+2.

4.3.3 Performance Evaluation of the PM Arrivals

The results suggest, that implementation of the proposed PM systems helps to earlier aircraft organization for landing (around 300 s to final), reduced spacing dispersion, and increased throughput, suggesting improved metering and spacing efficiency with the PM system. Analysis of the PM utilization indicates that in the current example the PM legs were not used very often due to low traffic, while the proposed design should be suitable for accommodating higher traffic load in the future. However, for the current traffic situation, the results obtained from our optimization framework indicate that a smaller PM implementation could be used to successfully manage the traffic situation at the airport. As additional work, we would, however, recommend the evaluation of other traffic scenarios, as one single case cannot cover all situations. Analyzing the results, we observe that the average total time and distance from the TMA entry and to the IF increased, when comparing optimized arrival routes with PM against the actual historical trajectories, while the average fuel consumption decreased by 5.0% (Table 2). The same observation also holds for the cluster performance analyzed individually for time and distance. In terms of fuel consumption, we observe the

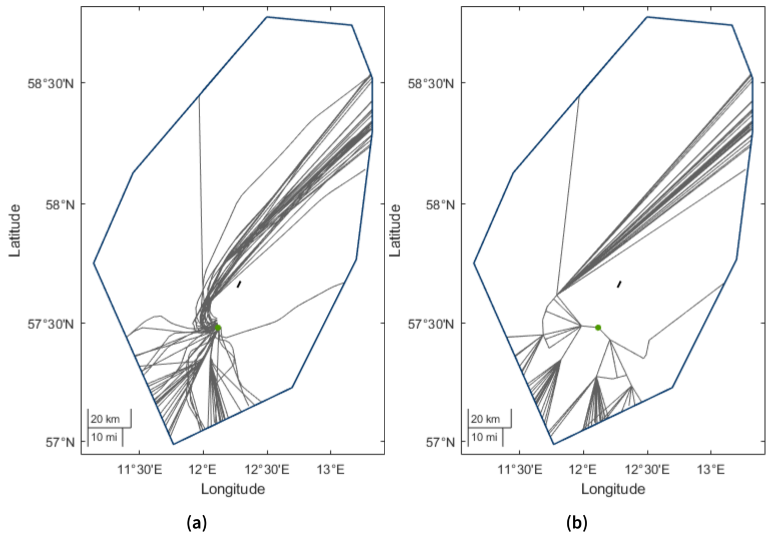

Figure 8. Actual (a) and optimized (b) trajectories for the 90 arriving flights on April 10, 2019.

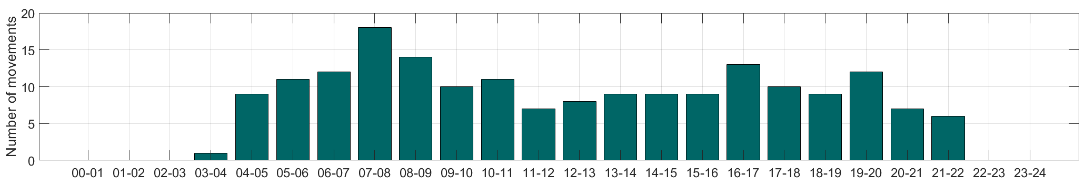

Figure 9. Number of movements for the optimized scenario with PM per hour, in April 10, 2019, defined as time of touchdown for arrivals and time of initiation of takeoff roll for departures.

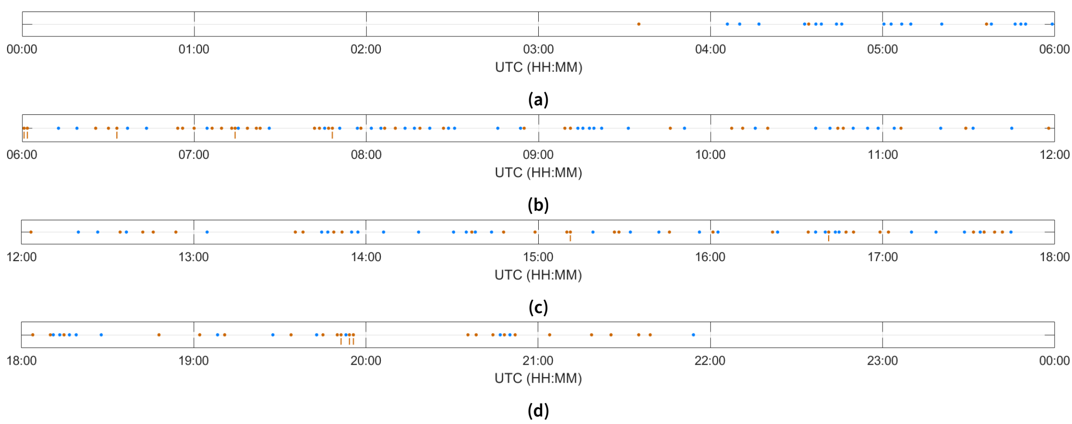

Figure 10. Timelines for 6-hour intervals (a-d) indicating the time of crossing the runway threshold or initiation of the takeoff roll, for arrivals and departures, respectively. Blue and orange dots represent departures and arrivals, respectively, while an orange line indicates that PM was used by the specific arriving flight.

decrease in all clusters except for Cluster 2, with the noticeable variation in the absolute values, where the only flight in Cluster 5 improved its fuel efficiency by 49%. The comparison results for the cluster-wise time, distance and fuel consumption are presented in Figure 11. Based on the results, we can conclude that the gain in the fuel efficiency cannot be attributed to decreased time or distance but to the improved vertical flight efficiency. A comparison between the vertical profiles of the actual and optimized trajectories is presented in Figure 12, where we observe flat, level-flight segments in the actual arrival trajectories. In Figure 12 (b), note the increase in number of aircraft having longer parts of their cruise phase within the TMA, compared to Figure 12 (a). This is partially because of a later top of descent (ToD), due to better vertical performance, and partially due to increased distance. The former holds especially for flights in cluster 2, for which the distance in TMA is relatively long. Hence, the later ToD results in an extended part of the cruise spent inside TMA, which may explain why the fuel efficiency of cluster 2 is not improved. Because of the noticeable variation in the number of flights per cluster (clusters 4 and 5 only containing one flight each), it is not possible to make a fair comparison of the change in performance between the different clusters.

Analysis of the vertical deviation from the reference profile metric calculated for the last 10 minutes of flight (or as long as the duration of the trajectory inside the TMA), in Figure 12 (c), confirms the observed inefficiencies in the actual profiles when compared to their reference optimized descents. Median deviation for the Clusters 1, 2, 3 and 5 are 4000, 7660, 3010 and 2190 $ft{\cdot}min$, respectively. We omit the results of clusters 4 and 5 since they contain only one flight each. The overall median vertical deviation taking all clusters into account is 4450 $ft{\cdot}min$.

Table 2. Change in time, distance and fuel consumption when comparing actual to optimized trajectories. Note that clusters 4 and 5 only contain one flight each.

	Cluster 1	Cluster 2	Cluster 3	Cluster 4	Cluster 5	Cluster 6	All Clusters
Number of flights	22	33	29	1	1	4	90
Time	+7.5%	+9.2%	+11.0%	+57.0%	+14.2%	+8.6%	+10.4%
Distance	+6.4%	+11.4%	+6.3%	+49.0%	+15.9%	+4.9%	+10.4%
Fuel	-16.0%	+5.9%	-12.2%	-4.3%	-49.0%	-15.5%	-5.0%

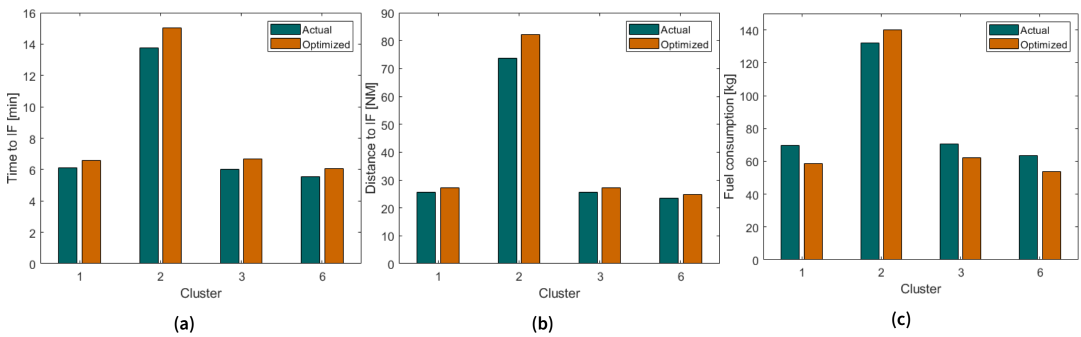

Figure 11. Cluster-wise time (a), distance (b) and fuel consumption (c) from TMA entry to IF, for actual and optimized trajectories. Note that clusters 4 and 5 are omitted due to low sample size.

Furthermore, we apply the sequencing and spacing evaluation framework to compare the actual and the optimized PM trajectories, Figures 13 and 14 respectively show the Minimum Time to Final heatmap, Spacing Deviation and Throughput metrics. Regarding Horizontal Spread, we observe a minor reduction of about 2% due to better organization of the arrival flows with PM procedures (16.1% for the actual versus 13.9% for the optimized trajectories). The maximum values of the Minimum Time to Final (a) are similar for the actual and optimized trajectories, 942 and 986 seconds respectively, however, the average values differ: 387 s for the actual and 494 for the optimized trajectories which is probably caused by the longer distance the aircraft fly in the TMA when adhering to the optimized routes.

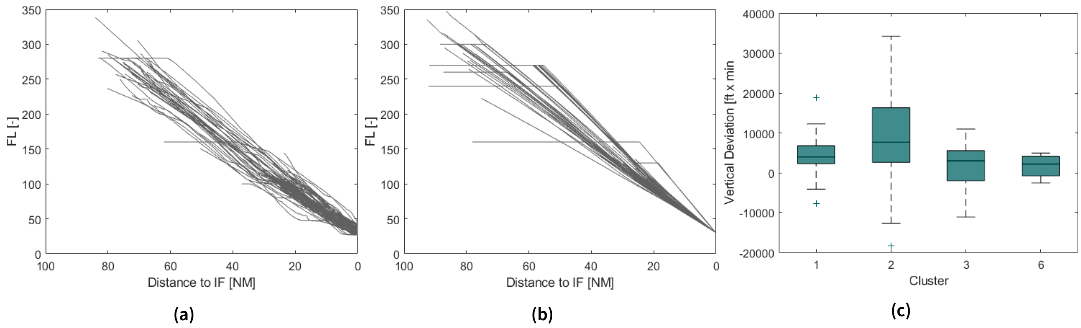

Figure 12. Actual (a) and optimized (b) vertical profiles, and vertical deviation for the last 10 min of flight (c), for the 90 arriving flights on April 10, 2019. Note that clusters 4 and 5 are omitted from (c) due to the low sample size.

The shapes of the Spacing Deviation figures (b) is very disperse around 900 seconds to final because we consider pairs of aircraft from various directions. The statistic values are similar for both scenarios with the 90th quantile width being 933 seconds for the actual and 984 seconds for the optimized trajectories. Despite no significant differences in the resulting values for the Spacing Deviation, we observe notable decrease in the evolution lines dispersion around 300 seconds to final for the optimized trajectories which implies that the aircraft were organized for final landing considerably earlier than in the case of the actual trajectories. The Throughput (c) confidence interval lines (blue) do not show any difference between the actual and the optimized trajectories but the increase in throughput values for the optimized scenario around 300 seconds to final matches with the dispersion decrease in Spacing Deviation figure. We observe that at approximately 300 s of minimum time to final in the heatmap for the optimized trajectories corresponds to the actual time when aircraft enter the PM sequencing legs. These results support that the introduction of the PM procedures accompanied by the optimized arrival scheduling noticeably improve the metering and spacing efficiency within TMA.

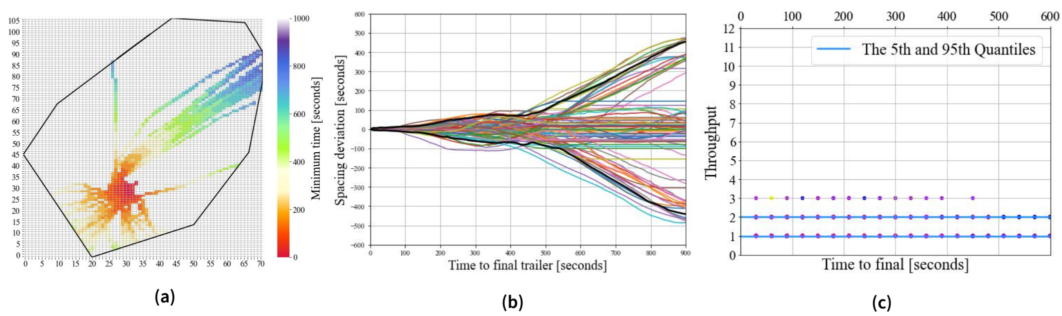

Figure 13. Minimum Time to Final heatmap (a), Spacing Deviation evolution curves (b), and Throughput plot (c) for the actual trajectories of the 90 arriving flights on April 10, 2019.

Additionally, we investigate the utilization of the proposed PM system, the results of the analysis presented in Table 3. We observe quite low utilization of the PM sequencing legs, provided by the relatively low traffic intensity even during the busiest day at Göteborg Landvetter. Out of the 90 flights in the studied subset, only 10 flights turned towards the merge point from other waypoint than the one by which they entered the PM system. Eight aircraft were detected by our algorithm since two of them turn immediately at the first extra waypoint, added in between existing ones. Hence, it is closest to the initial point and thus detected as not using PM. These results imply that, for the current operations at the airport, smaller PM system with shorter sequencing legs would

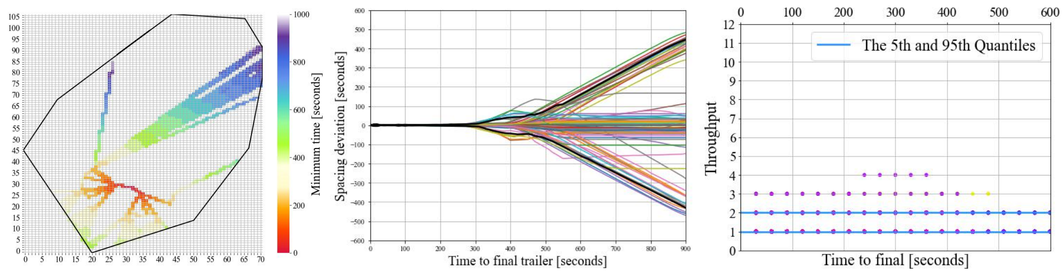

(a) (b) (c)

Figure 14. Minimum Time to Final heatmap (a), Spacing Deviation evolution curves (b), and Throughput plot (c) for the optimized trajectories of the 90 arriving flights on April 10, 2019.

be sufficient, while the proposed PM design should be desirable for future increase of the traffic volumes.

Table 3. PM Utilization Results

Percent Sequencing Legs	0%	20%	40%	60%	80%	100%
PM Utilization	91.1%	5.56%	1.11%	2.22%	0%	0%

5. Conclusions

In this study, we analyze the arrival flight trajectories to Göteborg Landvetter airport during the busiest month of the year 2019. The performance evaluation per flow was performed on six clusters. Analysis of the Spacing Deviation and Sequencing Effort metrics revealed that aircraft in Cluster 2 experience difficulties maintaining the given spacing intervals between the consecutive aircraft and thus require higher attention from the air traffic controllers. Furthermore, the vertical efficiency metric, Time Flown Level, revealed noticeable vertical inefficiencies in the Cluster 4, the cluster with the lowest number of arriving, which has to be investigated further. In addition, we observed similarity in the results for the Additional Time metric and the ASMA Additional Time metric, recently standardized by Eurocontrol.

Furthermore, we evaluated a PM system design for the Göteborg Landvetter TMA and scheduled 90 arrivals during the busiest day in 2019 along the new arrival procedures, applying the arrival optimization framework with the objective of minimizing the total fuel consumption. As expected, the evaluation of the optimized trajectories resulted in slightly longer time and distance the aircraft spent in TMA, but improved vertical efficiency as well as the desired decrease in fuel consumption (up to 49% for individual flights and 5% in average). In terms of sequencing and spacing, the actual and optimized trajectories show similar maximum values for Minimum Time to Final, but optimized routes lead to earlier aircraft organization for landing (around 300 s to final), reduced spacing dispersion, and increased throughput, suggesting improved metering and spacing efficiency with the Point Merge system. Analysis of the PM utilization indicates that in the current example the PM legs were not used very often due to low traffic, while the proposed design should be suitable for accommodating higher traffic load in the future. However, since our methodology evaluates only one specific scenario at a time, multiple runs with different traffic situations would be required in order to draw some final conclusion on what size PM system is suitable for Göteborg Landvetter airport, which is proposed future work. In addition, we would also apply the same methodology to the opposite runway, as well as explore the effects of introducing a time buffer to the separation requirements applied.

With this work, we have proven that the combination of the optimization and performance evaluation frameworks may serve as a tool for detailed assessment and fine-tuning of new arrival procedures, specifically adapted to the given airport and airspace.

Appendix 1. Selected Supplementary Equations and Pseudo-codes

Horizontal Spread (hs):

$$hs = (\frac{occupied\_cells}{all\_cells}) \times 100 \tag{6}$$

Fuel Consumption (F):

$$F = \delta \cdot \theta^{\frac{1}{2}} \cdot m \cdot g_0 \cdot a_0 \cdot L_{HV}^{-1} \cdot C_F \tag{7}$$

δ = pressure ratio, θ = temperature ratio, m = reference mass, g_0 = gravitational acceleration, a_0 = speed of sound at sea level, L_{HV}^{-1} = fuel lower heating value.

Minimum Time to Final:

Algorithm 1 Minimum Time to Final Pseudo-code

```
Require: F                                              ▷ flight data
Require: grid_x                                         ▷ number of cells horizontally
Require: grid_y                                         ▷ number of cells vertically
  function InitializeGrid(grid_x,grid_y,F)              ▷ Grid over trajectories return Grid
  end function
  function TimeToFinal(F)
     F(time_to_final) = F(time_landed) − F(time_now)
  end function
  cell_time = ∞                                         ▷ Initial value for each cell
  for all cell ∈ Grid do
     for all record ∈ cell do
        if record_time < cell_time then
           cell_time = record_time
        end if
     end for
  end for
  return min_time                                       ▷ Minimum Time to Final for each cell
```

Spacing Deviation (sd):

$$\mathrm{sd}(t) = \min\_time(\mathrm{trailer}(t)) - \min\_time(\mathrm{leader}(t - s_{\mathrm{rwy}})) \tag{8}$$

min_time = Minimum Time to Final value

Throughput:

Sequencing Effort (sf) :

$$sf(t) = sd(t) - sd(t_{final} - 30) \tag{9}$$

sd = Spacing Deviation

Additional Time (Ad_t):

$$Ad_t(i) = (ts_{max,i} - ts_{min,i}) - min\_time_{entry,i} \tag{10}$$

ts = timestamp, min_time = Minimum Time to Final value.

Algorithm 2 Throughput Pseudo-code

Require: F ▷ Flight data
Require: t_max ▷ Time horizon of calculation
$w = 300$ ▷ 5-minute time window
$s = 0, 30, 60, ..., 600$ ▷ Reference times
function $CreateIntervals(t\_max, w)$ **return** $Interval\_list$
end function
for all $I \in Interval\_list$ **do**
  $X = \sum_{i=1}(F(t)_i \in I)$
  for all s **do**
    $T = \sum_{i=1}(X(min\_time)_i \in (s, s+30))$
  end for
end for
return T ▷ Throughput in time

Author contributions

- First Author: Visualization, Investigation, Methodology, Software, Writing (Review and Editing)
- Second Author: Conceptualization, Supervision, Writing, Project Administration
- Third Author: Visualization, Investigation, Data curation, Writing-Original draft, Methodology, Software, Validation, Review and Editing, Formal Analysis, Resources

Funding statement

This research is supported by the Swedish Transport Administration (Trafikverket) and in-kind participation of LFV within the ODESTA-PM and TMAKPI projects.

Open data statement

In this work use open-source historical flight data of the OpenSky Network historical database.

Reproducibility statement

The initial datasets and scripts to reproduce results of the analysis are available at https://github.com/LucieSmetanova/Opensky_Symposium_2024.git.

References

[1] L. Boursier, B. Favennec, E. Hoffman, A. Trzmiel, F. Vergne, and K. Zeghal. "Merging arrival flows without heading instructions". In: *7th USA/Europe air traffic management R&D seminar.* 2007, pp. 1–8.
[2] DSNA/EUROCONTROL SESAR. *Point Merge Implementation - A quick guide, Edition 1.4.* 2021.
[3] Ö. S. Meric and O. Usanmaz. "A new standard instrument arrival: the point merge system". In: *Aircraft Engineering and Aerospace Technology* (2013).
[4] D. Ivanescu, C. Shaw, C. Tamvaclis, and T. Kettunen. "Models of air traffic merging techniques: evaluating performance of point merge". In: *9th AIAA Aviation Technology, Integration, and Operations Conference (ATIO) and Aircraft Noise and Emissions Reduction Symposium (ANERS).* 2009, p. 7013.

[5] M. Liang, D. Delahaye, and P. Maréchal. “Potential operational benefits of multi-layer point merge system on dense TMA operation hybrid arrival trajectory optimization applied to Beijing capital international airport”. In: *Proceedings of the 7th International Conference on Research in Air Transportation.* 2016.

[6] DSNA/EUROCONTROL SESAR. *P05.06.02 - D57 - CDO at Orly Real-time Simulations Validation Report.* 2015.

[7] Wilde J.M. *Implementing point merge system based arrival management at Amsterdam Airport Schiphol. MS thesis.* http://repository.tudelft.nl/. August 2018.

[8] M. Liang, D. Delahaye, and P. Maréchal. “A framework of point merge-based autonomous system for optimizing aircraft scheduling in busy TMA”. In: *5th SESAR Innovation Days, Bologna, Italy* (2015).

[9] SONER Demirel. “Comparison of RECAT-EU and ICAO wake turbulence category on the Point Merge System”. In: *The Aeronautical Journal* 127.1315 (2023), pp. 1623–1637.

[10] H. Hardell, T. Polishchuk, and L. Smetanova. “ Fine-Grained Evaluation of Arrival Operations.” In: *SIDs.* 2020.

[11] H. Hardell, A. Lemetti, T. Polishchuk, and L. Smetanová. “Evaluation of the Sequencing and Merging Procedures at Three European Airports Using Opensky Data”. In: *Engineering Proceedings* 13.1 (2022), p. 13.

[12] H. Hardell, T. Polishchuk, and L. Smetanová. “Automated Traffic Scheduling in TMA with Point Merge to Enable Greener Descents”. In: *10th International Conference on Research in Air Transportation (ICRAT), Tampa, June 19-23, 2022.* 2022.

[13] H. Hardell, A. Lemetti, and T. Polishchuk. “Performance Evaluation of the Arrival Operations in the Terminal Area”. In: *33rd Congress of the International Council of the Areonautical Sciences (ICAS), Stockholm, September 4-9, 2022.* 2022.

[14] Swedavia. *Flygstatistik.* https://www.swedavia.se/om-swedavia/statistik/. last accessed on 13.03.2025. 2025.

[15] *Opensky Network.* https://opensky-network.org/. last accessed on 11.02.2022.

[16] Anastasia Lemetti, Henrik Hardell, and Tatiana Polishchuk. “Arrival flight efficiency in pre- and post-Covid-19 pandemics”. In: *Journal of Air Transport Management* 107 (2023), p. 102327. ISSN: 0969-6997. DOI: https://doi.org/10.1016/j.jairtraman.2022.102327. URL: https://www.sciencedirect.com/science/article/pii/S0969699722001466.

[17] A. Lemetti, T. Polishchuk, H. Hardell, K. Zeghal, and L. Smetanová. “Towards a Comprehensive Characterization of the Arrival Operations in the Terminal Area.” In: *SIDs.* 2021.

[18] H. Hardell, A. Lemetti, T. Polishchuk, and L. Smetanová. “Performance Characterization of Arrival Operations with Point Merge at Oslo Gardermoen Airport”. In: *15th USA/Europe Air Traffic Management Research and Development Seminar (ATM2023), Savannah, Georgia, June 5-9, 2023.* 2023.

[19] EUROCONTROL Mesón-Mancha Sara. *Additional ASMA time performance indicator document, Technical Documentation, Edition 1.0.* 2023.

[20] Henrik Hardell, Tatiana Polishchuk, and Lucie Smetanová. “Arrival Optimization with Point Merge in a Dual-runway Environment”. In: *SESAR Innovation Days, Sevilla, Spain.* 2023. URL: https://api.semanticscholar.org/CorpusID:267394290.

[21] *Copernicus Climate Change Service (C3S) Data Store, European Centre for Medium-Range Weather Forecasts (ECMWF).* https://cds.climate.copernicus.eu. last accessed on 04.03.2025.

[22] EUROCONTROL. *User Manual for the Base of Aricraft Data (BADA) Family 4.* 2014.

[23] Richard de. Neufville and Amedeo R. Odoni. *Airport Systems. Planning, Design, and Management.* Mc Graw Hill, 2013.

[24] LFV. *GÖTEBORG/Landvetter ILS or LOC RWY 03.* https://aro.lfv.se/Editorial/View/9097/ES_AD_2_ESGG_5-1_en. last accessed on 25.02.2025. 2021.

[25] Gurobi. *Gurobi Optimizer*. https://www.gurobi.com/solutions/gurobi-optimizer/. last accessed on 04.03.2025. 2025.